Food Hydrocolloids 125 (2022) 107400

Contents lists available at ScienceDirect

Food Hydrocolloids

journal homepage: www.elsevier.com/locate/foodhyd

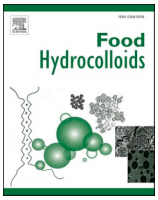

Napins and cruciferins in rapeseed protein extracts have complementary roles in structuring emulsion-filled gels

Eleni Ntone [a,b,1], Remco Kornet [b,c,1], Paul Venema [c], Marcel B.J. Meinders [d], Erik van der Linden [c], Johannes H. Bitter [a], Leonard M.C. Sagis [c], Constantinos V. Nikiforidis [a,*]

[a] Biobased Chemistry and Technology, Wageningen University and Research, Bornse Weilanden 9, PO Box 17, 6708 WG, Wageningen, the Netherlands
[b] TiFN, P.O. Box 557, 6700 AN, Wageningen, the Netherlands
[c] Laboratory of Physics and Physical Chemistry of Foods, Wageningen University, Bornse Weilanden 9, 6708 WG, Wageningen, the Netherlands
[d] Food and Biobased Research, Wageningen University and Research Centre, P.O. Box 17, Bornse Weilanden 9, 6708 WG, Wageningen, the Netherlands

ARTICLE INFO

Keywords:
Emulsion-filled gels
Rapeseed proteins
Plant proteins
Protein gels
Rheology
Functionality

ABSTRACT

We investigated the complementary roles of napins and cruciferins present in a rapeseed protein mixture (RPM) in structuring emulsion-filled gels (EFGs). Napins are small molecular weight albumins with high interfacial activity, while cruciferins are high molecular weight globulins that form gels upon heat-induced gelation. The role of napins is to stabilize the emulsion droplets, while cruciferins, which were previously found to interact with the adsorbed napin interfacial layer, can build the protein gel network around the droplets. The effects of oil concentration (0–30 wt%) and pH (5 and 7) on the rheological and microstructural properties of EFGs were investigated. In the absence of oil, at pH 5, due to low protein solubility, RPM formed a heterogeneous network built of protein aggregates. At pH 7, RPM was more soluble and formed a homogeneous network built of strand-like protein structures with higher gel firmness. In the presence of emulsion droplets, the gel firmness increased, with a more pronounced reinforcement at pH 5 compared to pH 7. The type of gel network did not change by the presence of emulsion droplets neither at pH 5 nor at pH 7, as suggested from confocal microscopy and the unchanged response to large deformation. This implies that oil did not really change the protein network structure. The emulsion droplets, being stiffer than the protein matrix, and being integrated in the structural matrix, increased the gel firmness. This research shows that the presence of two different proteins with complementary roles in a less purified protein extract, provides a single protein ingredient suitable for structuring food emulsion-filled gels.

1. Introduction

Traditionally, plant protein extraction processes focus on high protein purity and yield (Berghout, Pelgrom, Schutyser, Boom, & Van Der Goot, 2015), although often there is a trade-off between purity and yield (Loveday, 2020; Tamayo Tenorio, Kyriakopoulou, Suarez-Garcia, van den Berg, & van der Goot, 2018). In recent years, more attention has been paid to the environmental impact of plant protein extraction– such as energy and water usage – and to the effect of protein extraction and purity on functionality (Assatory, Vitelli, Rajabzadeh, & Legge, 2019; Lie-Piang, Braconi, Boom, & van der Padt, 2021; Schutyser & van der Goot, 2011; Van Der Goot et al., 2016). It has been reported that less purified plant protein extracts yield equal or better foaming, emulsifying, and gelling properties compared to highly purified plant protein extracts for a variety of plant sources. Examples of such plant sources include soy (Peng, Kersten, Kyriakopoulou, & van der Goot, 2020), peas (Sridharan, Meinders, Bitter, & Nikiforidis, 2020; Fuhrmeister & Meuser, 2003; Kornet et al., 2021), chickpeas (Papalamprou, Doxastakis, Biliaderis, & Kiosseoglou, 2009), sunflower seeds (Karefyllakis, Octaviana, van der Goot, & Nikiforidis, 2019) and rapeseeds (Yang et al., 2021). The functionality of the less purified plant protein extracts can be ascribed to the different functionalities of the proteins in the mixture and the prevention of process-induced protein interactions (e.g., leading to aggregation).

* Corresponding author. Biobased Soft Materials Biobased Chemistry and Technology, Wageningen University, P.O. Box 17, 6708 WG, Wageningen, the Netherlands.
E-mail address: costas.nikiforidis@wur.nl (C.V. Nikiforidis).
[1] These authors have contributed equally to this work.

https://doi.org/10.1016/j.foodhyd.2021.107400
Received 3 August 2021; Received in revised form 2 November 2021; Accepted 23 November 2021
Available online 24 November 2021

Rapeseeds are a potential source of functional proteins for foods; however, the current oilseed valorisation process, which includes defatting, heating and use of organic solvents, has a tremendous impact the extractability and functional properties of the proteins (Fetzer, Herfellner, Stäbler, Menner, & Eisner, 2018). As a result, rapeseed proteins are underutilized in food applications (Chmielewska et al., 2020; Mosenthin et al., 2016). In previous work we showed that using an alternative extraction method, where no defatting is applied, and an aqueous extraction is followed, the physicochemical and functional properties of the proteins can be preserved (Ntone, Bitter, & Nikiforidis, 2020; Ntone et al., 2021). This paves the path to explore the functionality potential of rapeseed proteins that could initiate their use in foods.

Rapeseeds contain two types of storage proteins, named napins and cruciferins. Napins are small molecular weight albumins (15–17 kDa), which are soluble in a wide pH range and show high heat stability (with a denaturation temperature $T_d \geq 100$ °C) (Wanasundara, Abeysekara, McIntosh, & Falk, 2012). The hydrophobic domains of napins are concentrated on one side of the protein, reminiscent of a Janus particle (Ntone et al., 2021). Cruciferins, are globulins with a high molecular weight (300 kDa) and a hexamer structure consisting of two trimers (Perera, McIntosh, & Wanasundara, 2016). The hydrophobic domains of cruciferins are widely distributed over the protein's surface, and also buried within the cruciferin trimers (Perera et al., 2016). The hexamer structure of cruciferins is more susceptible to structural changes and unfolding upon heating and pH changes compared to napins (Wanasundara et al., 2012; Wanasundara, McIntosh, Perera, Withana-Gamage, & Mitra, 2016).

In a previous work, we showed that a less purified rapeseed protein mixture (RPM) with 40 wt% protein content and all storage proteins present (napins and cruciferins) –obtained from non-defatted seeds after aqueous alkaline extraction and subsequent separation of proteins from oil– can form stable emulsions at pH 7. Based on previous research on the interfacial properties of RPM, when RPM was used as an emulsifier, napins were found to govern the interface of the emulsion droplets, while cruciferins weakly interacted with the primary adsorbed layer (Ntone et al., 2021). Napins exhibit higher interfacial activity than cruciferins (Krause & Schwenke, 2001), probably due to their structure, in which the hydrophobic domains are concentrated at one side of the protein structure (Ntone et al., 2021). However, it has been reported that cruciferins have better gelling properties, as they form firmer gels than napins upon heat-induced gelation (Schwenke, Dahme, & Wolter, 1998; Tan, Mailer, Blanchard, Agboola, & Day, 2014; C.; Yang, Wang, Vasanthan, & Chen, 2014).

Considering the emulsifying properties of napins and gelling properties of cruciferins, we anticipate the two proteins present in RPM can have complementary functionalities in structuring emulsion-filled gels (EFGs). Such EFG's are protein gels with embedded emulsion droplets (Dickinson, 2012). Different kinds of food products such as set yoghurt, fresh cheese, puddings, dairy desserts and sausages can be categorized as protein emulsion-filled gels (Sala, van Vliet, Cohen Stuart, Aken, & van de Velde, 2009 a). When RPM is used to structure EFGs, napins can stabilize the emulsion droplets, and cruciferins which weakly interact with napins at the interface (Ntone et al., 2021), can build the protein gel network, and both proteins interacting at the droplet-matrix contact sites.

Depending on the interactions on the two proteins on droplet-matrix contact sites, EFGs can show different rheological characteristics (Dickinson, 2014; Genovese, 2012); When the droplet interface interacts with the matrix, as in the case of napins with cruciferins (Ntone et al., 2021), the droplets can act as active fillers, and potentially reinforce the gel structure. Such interactions are often seen in case the droplets are stabilized by proteins (Chen, Dickinson, & Edwards, 1999; Dickinson, 2012), whereas surfactant-coated oil droplets usually do not or only weakly interact with the protein matrix (Chen & Dickinson, 1998; Dickinson & Hong, 1995; McClements, Monahan, & Kinsella, 1993). Apart from the droplet-matrix interactions, the rheological characteristics of EFGs depend on the protein and oil content, and the stiffness of the droplets and the matrix (Dickinson, 2014; Genovese, 2012).

In this work we used the less purified rapeseed protein mixture (RPM) containing napins and cruciferins to structure EFGs, which were studied using bulk rheology and confocal microscopy. The effect of oil concentration and pH on the rheological properties and microstructure of the EFGs was investigated. Exploiting the potential complementary roles of the different proteins present in plant extracts, may lead to the employment of protein mixtures with multiple functions. Using a less purified extract with multiple functions, instead of multiple single function ingredients, can reduce the extraction and processing steps in the food chain, increasing the overall sustainability of plant-based foods.

2. Material and methods

2.1. Materials

Untreated Alize rapeseeds (stored at −18°C) were used for the extraction of the protein mixture. Rapeseed oil was kindly provided by Nutricia Research B.V. All other chemicals were of analytical grade and obtained from Sigma Aldrich (Steinheim, Germany). All samples were prepared with demineralized water. All samples and subsequent analyses were performed in duplicates.

2.2. Methods

2.2.1. Extraction of the rapeseed protein mixture

The rapeseed protein mixture (RPM) was extracted as described before (Ntone et al., 2020). Dehulled rapeseeds were soaked in deionized water at a ratio of 1:8 (w/w) at pH 9.0 (adjusted with 0.5 M NaOH solution) under continuous stirring with a head stirrer (EUROSTAR 60 digital, IKA, Staufen, Germany) at room temperature (~20°C) for 4 h. Afterwards, the dispersion was blended with a kitchen blender (HR2093, Philips, Netherlands) for 2 min at maximum speed. To separate the solids from the liquid phase, the resulting slurry was filtered using a twin-screw press (Angelia 7500, Angel Juicer, Naarden, The Netherlands). The filtrate was collected, the pH was adjusted to pH 9.0, and centrifuged (10,000 g, 30 min, 4°C) (Sorvall Legend XFR, ThermoFisher Scientific, Waltham, MA, USA). A cream layer (oleosome-rich), a serum (protein mixture (RPM)) and a pellet (fibre-rich) were obtained. The serum was freeze-dried (Alpha 2–4 LD plus, Martin Christ Gefriertrocknungsanlagen GmbH, Osterode am Harz, Germany) to obtain an RPM powder, which was stored at −18°C until further use.

2.2.2. Characterization of the rapeseed protein mixture

2.2.2.1. Protein content. The protein content of the freeze-dried RPM was determined with the Dumas method (FlashEA 1112 Series, Thermo Scientific, Waltham, Massachusetts, US); D-methionine (≥98%, Sigma Aldrich, Darmstadt, Germany) was used as a standard and as a control. Cellulose (Sigma Aldrich, Darmstadt, Germany) was used as blank. A nitrogen–protein conversion factor of 5.7 - calculated based on amino acid sequence – was used.

2.2.2.2. Protein profile of supernatant after centrifugation. The qualitative analysis of the proteins present in the supernatant after removal of large aggregates from RPM dispersions at pH 5 or pH 7 was carried out using sodium dodecyl sulphate–polyacrylamide gel electrophoresis (SDS-PAGE), to provide a protein profile. First, the RPM was dispersed in deionized water (standardized at 0.5 wt% protein content), the pH was adjusted to pH 5 or pH 7 using 0.5 M NaOH or HCl and the dispersions were stirred at room temperature for 2 h with a magnetic stirrer at 300 rpm (2mag magnetic e motion, 2mag AG, Munich, Germany), followed by centrifugation (10,000 g, 30 min, 20°C) (Sorvall Legend XFR,

ThermoFisher Scientific, Waltham, MA, USA). A pellet, a clear serum and a thin cream layer of oleosomes at the surface were obtained. The clear serum was carefully separated and mixed with a sample buffer (NuPAGE® LDS, Thermo- Fisher, Landsmeer, the Netherlands) to achieve a final protein concentration of 1.0 mg/mL. Then, 10.0 μL of a protein marker (PageRuler™ Prestained Protein Ladder, 10–180 kDa, ThermoFisher, Landsmeer, the Netherlands) and 15 μL of the sample were loaded onto the gel (NuPAGE® Novex® 4–12% Bis-Tris Gel, ThermoFisher, Landsmeer, the Netherlands). MES running buffer (NuPAGE® MES SDS Running Buffer, ThermoFisher, Landsmeer, the Netherlands) was used. The gel was washed with water and stained (Coomassie Brilliant Blue R-250 Staining Solution, Bio-Rad Laboratories B.V., Lunteren, the Netherlands) overnight under gentle shaking. Thereafter, the gel was washed with demineralized water and destained (destaining solution of 10% ethanol and 7.5% acetic acid in deionized water) overnight under gentle shaking. Images of the gels were taken using a camera.

2.2.3. Preparation of emulsions used in emulsion-filled gels

To obtain emulsion-filled gels with final concentrations of 10.0, 20.0 and 30.0 wt% oil, emulsions of 11.6, 22.7 and 33.5 wt% oil (of total mass) were prepared using RPM. To ensure a similar individual droplet size of the emulsion droplets at different oil concentrations, the protein to oil ratio was kept at 1:14.3 (w/w) (based on protein content of RPM) as well as the number of passes through the homogenizer (N = 5), and the homogenization pressure was adjusted. In Table 1 the homogenization pressures and the protein concentrations used for the different emulsions are summarized. The emulsions were prepared as previously reported (Ntone et al., 2021). First, RPM was dispersed in deionized water (aqueous phase) at the corresponding protein concentration, the pH was adjusted to 7.0 and the dispersions were stirred for 2 h at room temperature (~20°C) with a magnetic stirrer at 300 rpm (2mag magnetic e motion, 2mag AG, Munich, Germany) to allow hydration and solubilization of the proteins. Thereafter, a pre-homogenization step was applied using a shear homogenizer (Ultra-Turrax, IKA®, Staufen, Germany) set to 8000 rpm for 30 s. Next, the rapeseed oil was slowly added to the dispersion and sheared for 1 min at 10,000 rpm. The coarse emulsions was further processed with a high-pressure homogenizer (GEA®, Niro Soavi NS 1001 L, Parma, Italy) for 5 passes.

To determine the individual droplet size of the emulsions, 1.0 wt% SDS was added to emulsion aliquots used for measuring the size, before the measurement, at a ratio of 1:1 (v/v), and the individual droplet size of the emulsions was measured using a Bettersizer S3 Plus (3P Instruments GmbH & Co. KG, Odelzhausen I Germany).

SDS is a low molecular weight surfactant whose role is to break protein-protein hydrophobic interactions (Reynoldst & Tanford, 1970) and it was added to prevent extensive hydrophobic interactions between the emulsion droplets that lead to droplet aggregation. This allowed the measuring of the actual individual droplet size instead of the droplet aggregate size. The individual droplet size expressed as volume ($d_{4,3} = \Sigma n_i d_i^4/\Sigma n_i d_i^3$) and surface ($d_{3,2} = \Sigma n_i d_i^3/\Sigma n_i d_i^2$) mean diameter (where n_i is the number of droplets with a diameter of d_i) is also given in Table 1.

Table 1
Oil concentration, protein concentration, homogenization pressure (bar) and individual droplet size of the emulsions prepared at pH 7 in deionized water, used for the preparation of the emulsion-filled gels (±standard deviation).

Oil (wt% of total)	Protein concentration (wt% of total)	Homogenization pressure (bar)	$d_{4,3}$ (μm)	$d_{3,2}$ (μm)
11.6	0.8	250	1.7 ± 0.0	1.5 ± 0.0
22.7	1.6	300	1.9 ± 0.5	1.4 ± 0.2
33.5	2.3	350	2.2 ± 0.5	1.6 ± 0.1

2.2.4. Preparation of emulsion-filled gels

The emulsion-filled gels (EFGs) containing different oil concentrations (10.0, 20.0 and 30.0 wt% of total mass) were prepared by dispersing RPM powder in the emulsions of different oil concentrations (prepared as described in section 2.2.3), resulting in protein-enriched emulsions. RPM was added to the emulsions to achieve a concentration of 15.0 wt% in the aqueous phase of each emulsion system. A reference sample (gel matrix) in which RPM was dispersed in water at the same concentration was also prepared. The pH of the systems was adjusted to pH 5 or pH 7 and the samples were left for 2h under continuous stirring using a magnetic stirrer at 200 rpm (2mag magnetic e motion, 2mag AG, Munich, Germany) to allow hydration and solubilization of the added proteins. Thereafter, the samples were stored at 4°C until the next day when they were heated to temperatures above the protein denaturation temperatures, in the rheometer, to induce gelation.

2.2.5. Microstructural visualization

To visualize the microstructure of the emulsion-filled gels (EFGs), the protein-enriched emulsions were stained with Nile red (1 mg/mL dissolved in ethanol) and Fast green (1 mg/mL dissolved in deionized water) at a sample to dye ratio of 1:200 for the oil and protein, respectively. The stained samples were transferred to sealed glass chambers (Gene frame 65 μl adhesives, Thermo Fisher Scientific, United Kingdom). The frames were placed in a water bath (100°C, 15 min). Afterwards, the samples were cooled immediately with water to room temperature. The samples were visualized using a Confocal Laser Scanning Microscope with a water immersion objective at 63× magnification (Leica SP8-SMD microscope, Leica Microsystems, Wetzlar, Germany). Nile red was excited at 488 nm and the emission was measured between 500 and 600 nm and Fast green was excited at 633 nm and the emission was measured between 650 and 750 nm. The dyes were excited and emitted in a sequential mode using a white light laser.

2.2.6. Shear viscosity measurements

The shear viscosity of the protein dispersions (15 wt% RPM) was measured with an MCR302 rheometer (Anton Paar, Graz, Austria). The samples were transferred to a double-gap geometry (DG 26.7). The steady-shear viscosities were measured for 2 min, with incrementing shear rates of 0.1, 0.5, 1, 5, 10, 50, 100 s^{-1} followed by decrementing shear rates of 50, 10, 5, 1, 0.5 and 0.1 s^{-1}. The temperature was kept constant at 20°C. The experiment was set up in this way to determine the shear dependency (e.g. shear-thinning behaviour) and to determine whether the dispersions showed thixotropy and/or hysteresis.

2.2.7. Small amplitude oscillatory shear (SAOS) rheology

The samples were studied on their gelling behaviour with an MCR302 rheometer (Anton Paar, Graz, Austria). The protein-enriched emulsions were transferred to a concentric cylinder (CC-17). A sand-blasted geometry was used, to reduce the chance of wall-slip. A solvent-trap was placed on top of the cylinder, to prevent solvent evaporation upon heating. The sample was heated from 20°C to 100°C with a rate of 3°C/min, kept at 100°C for 10 min, and cooled to 20°C with a rate of 3°C/min. To make sure that no gel maturation took place, the sample was kept at 20°C for another 5 min. Throughout this temperature sweep, an oscillatory deformation was imposed at a constant frequency of 1 Hz and a strain of 1%, which fell within the linear viscoelastic (LVE) regime of the gel. The response was recorded and the resulting G' and G'' were determined by the Rheocompass Software (Anton Paar, Graz, Austria). All samples were measured in duplicate.

2.2.8. Large amplitude oscillatory shear (LAOS) rheology

After the temperature sweep, the emulsion-filled gels were characterized for their non-linear rheological behaviour, using the same rheometer and geometry as for the SAOS measurements. This type of experiment (i.e., LAOS) was conducted to obtain a more detailed view on the breakdown behaviour of the gels, and to link those observations

to structural properties.

In these measurements, the strain was increased logarithmically from 0.1 to 1000% at a constant frequency of 1 Hz and a temperature of 20°C. The end of the LVE regime was defined as the strain at which the G' had decreased to 90% of its original value, which was expressed as the critical strain.

For each imposed strain amplitude, the oscillating strain, stress and shear rate signals were recorded. This data was normalized, and elastic and viscous Lissajous plots were constructed. The elastic and viscous contributions at each strain amplitude were calculated by the Rheocompass Software (Anton Paar, Graz, Austria), and plotted in the Lissajous figures.

The area enclosed within the Lissajous curves represents the energy dissipated (E_d) per unit volume during one oscillatory cycle. This information can be summarized by plotting the energy dissipation ratio as a function of strain amplitude. The energy dissipation ratio (Φ) is the ratio of the dissipated energy at a certain strain amplitude (E_d) over the energy dissipated by a perfect plastic material ($E_{d(pp)}$) (Schreuders, Sagis, Bodnár, Erni, Boom et al., 2021). The energy dissipation ratio is related to the loss modulus (G'') and the maximum stress (σ_{max}) at a given strain amplitude (γ_0) by Eq. (1) (Ewoldt, Winter, Maxey, & McKinley, 2010):

$$\Phi = \frac{E_d}{(E_d)_{pp}} = \frac{\pi G'' \gamma_0}{4\sigma_{max}} \quad (1)$$

2.2.9. Statistical analysis

All measurements were performed at least in duplicate. The standard deviations of the mean values were calculated and used to express the variability. Claims regarding statistical differences were supported by one-way ANOVA analysis. Significance was defined as $P < 0.05$.

3. Results and discussion

Rapeseed protein mixtures (RPM) were extracted from non-defatted and dehulled rapeseeds following our previously reported aqueous extraction process (Ntone et al., 2020), and used as starting material to prepare the emulsion-filled gels. The followed extraction protocol aimed to simultaneously extract napins and cruciferins and maintain the protein physicochemical properties. With this extraction method process-induced alterations in protein physicochemical properties (i.e. solubility) with impact on functionality (McCurdy, 1990; Ozdal, Capanoglu, & Altay, 2013; Rawel, Meidtner, & Kroll, 2005; Sari, Mulder, Sanders, & Bruins, 2015), a commonly reported drawback of commercial extraction methods, are avoided. This allows to explore the potential of rapeseeds proteins to be used as functional ingredients for foods.

The resulting rapeseed protein mixture (RPM) had an average protein content of 39.4 ± 0.4 wt% (as determined from different batches extracted for this study), and consisted of napins and cruciferins in a mass ratio of 1:1. As no defatting of the seeds was applied, lipids were also present in the protein extract in their natural structures (oleosomes). The approximate composition of the remaining non-protein molecules, based on previous studies, was 12.0 wt% oleosomes, 6.0 wt % free phenolic compounds, 8.0 wt% ash and 35.0 wt% polysaccharides (Ntone et al., 2020, 2021).

3.1. Physicochemical properties of RPM dispersions

For the use of RPM as a dual-purpose ingredient in emulsion-filled gels, it was needed to understand the physicochemical properties of the protein network (matrix) and the embedded emulsion droplets. Regarding the matrix properties, we first studied RPM in dispersions at pH 5 and pH 7. A concentration of 15.0 wt% RPM (which corresponds to 5.9 wt% protein) in EFGs was chosen, as from preliminary data (not shown here) this concentration was found to be sufficient for gel formation. Thereafter, the emulsion droplets stabilized with RPM were characterized.

First the effect of the solubility of rapeseed proteins on the shear viscosity of RPM aqueous dispersions (15.0 wt% RPM) as a function of pH was studied. Fig. 1 shows the viscosity of RPM dispersions as a function of shear rate at pH 5 and pH 7. The viscosity of the protein dispersion at pH 7 hardly changed as a function of shear rate, closely resembling Newtonian behaviour. At pH 5 the viscosity was higher and showed a decrease with increasing shear, indicating shear thinning behaviour. Both at pH 5 and pH 7 the backward loop showed the same shear-dependency of viscosity as the forward loop, indicating that there was no hysteresis and thixotropy observed for the dispersions. Newtonian-like behaviour is typically seen for water and oil (Braun & Rosen., 2013) and may indicate the absence of large or interacting molecules. The absence of hysteresis at pH 7 implies the absence of larger particles and is consistent with the higher solubility of RPM at pH 7 compared to pH 5 (Ntone et al., 2020). Previously it has been shown that the solubility of rapeseed proteins is lower at pH 5 compared to pH 7 (i.e. 40 vs 70 wt%) (Gerzhova, Mondor, Benali, & Aider, 2016; Ntone et al., 2021; Wanasundara et al., 2012). The reduced solubility at pH 5 could be attributed to the fact that pH 5 is close to the zero-charge point (ζ-potential around −5 mV at pH 5 vs −15 mV at pH 7) (Ntone et al., 2020), leading to low electrostatic forces present, and allowing hydrophobic attractive forces to dominate the system, resulting in aggregation. The protein aggregates are expected to have a more open structure and therefore a larger specific volume in comparison to the soluble (non-aggregated, hard sphere like) protein molecules. As a result, the formed protein aggregates at pH 5, when dispersed in aqueous phase, lead to a higher viscosity, compared to the soluble proteins. This is supported by the observed shear-thinning behaviour, which implies that larger – and possibly interacting – particles are present at rest. These protein particles or aggregates either align with the flow or break down with increasing shear. In the latter case, the particles must recover in timescales shorter than in which the viscosity is measured at a specific shear rate, as no hysteresis was observed.

The different solubility of proteins at the pH 5 and pH 7 is also linked with different gelling behaviour of rapeseed proteins (Wanasundara et al., 2016). It has been previously reported that napins are soluble at a broader pH range compared to cruciferins, for which solubility increases by increasing pH (Perera et al., 2016), and with minimal solubility reported close to pH 4–5 (Cheung, Wanasundara, & Nickerson, 2014; Withana-Gamage, Hegedus, Qiu, & Wanasundara, 2015). Therefore, to determine the type of proteins present in the aggregates at each pH, the larger insoluble protein aggregates were removed using centrifugation,

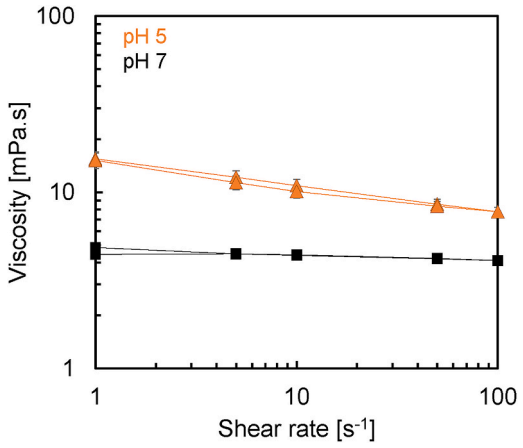

Fig. 1. Shear viscosities in forward and backward loop of 15.0 wt% rapeseed protein mixture (RPM) dispersions at pH 5 and 7. The shear rate was increased (and decreased) stepwise. All samples were measured in duplicate and the standard deviations are represented by the error bars (with some of them smaller than the data points).

and the protein composition of the supernatant was determined using electrophoresis. Fig. 2 shows the electrophoregram (SDS-PAGE) of the proteins present in the supernatant of centrifuged RPM dispersions prepared at pH 5 and pH 7. Both at pH 5 and pH 7, we identified a band around 17 kDa, which is related to napins (Monsalve, Lopez-otin, Villalba, & Rodriguez, 1991). At pH 7 several bands in the range of 20–70 kDa were also present, corresponding to cruciferins (Dalgalarrondo, Robin, & Azanza, 1986). The band representing napins shows a similar intensity at pH 5 and 7, indicating that the solubility of napins is not affected in this pH range. The cruciferin bands were more pronounced at pH 7 than at pH 5, indicating that cruciferins formed larger insoluble aggregates at pH 5, which were centrifuged out and resulted in a lower band intensity. The lower solubility of cruciferins at this pH could be a result of the nearly zero net charge of cruciferins close to pH 5 (Tan et al., 2014), which probably cause the formation of cruciferin aggregates (Perera et al., 2016). In addition, the phenolic compounds (i.e. sinapic acid) present in RPM can induce aggregation, particularly close to the isoelectric point, leading to further protein aggregation (Ozdal et al., 2013; Rubino, Arntfield, Nadon, & Bernatsky, 1996).

3.2. Properties of emulsion droplets used in EFGs

The emulsion droplet size is one important parameter that influences the rheological and mechanical properties of EFGs (Farjami & Madadlou, 2019; Geremias-Andrade, Souki, Moraes, & Pinho, 2016; Sala, van Vliet, Cohen Stuart, van de Velde, & van Aken, 2009 b). To exclude any effect of droplet size, we standardized the mean emulsion droplet size independently of the oil concentration, by keeping the same protein to oil ratio and adjusting the homogenization pressure as summarized earlier in Table 1. The droplet size distribution of the emulsions was similar for all the emulsions independent of the oil concentration, with a mean individual droplet size ($d_{4,3}$) around 2 μm (Table 1) (size not significantly different between samples as $P > 0.05$).

Another important parameter that affects the rheological properties of EFGs is the interaction between the emulsion droplets and the protein matrix, which is influenced by the interfacial composition of the droplets (Chen & Dickinson, 1999; Farjami & Madadlou, 2019; Geremias-Andrade et al., 2016). All the emulsions were prepared (prior to the addition of 15.0 wt% RPM) at pH 7, as from our previous research we know that when using RPM as an emulsifier at pH 7, the interface of the droplets is dominated by napins, while cruciferins weakly interact with the primary adsorbed layer (Ntone et al., 2021). Based on the results of the previous research on the interfacial properties of RPM, the reported interfacial composition results in a viscoelastic interface, with an elastic modulus (E_d') of approximately 25 mN/m (at 5% amplitude).

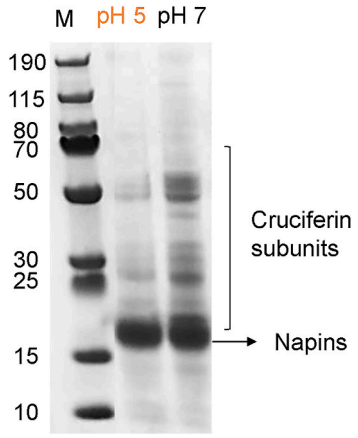

Fig. 2. Electrophoregram (SDS-PAGE) under non-reducing conditions of the proteins present at supernatant of RPM dispersions (0.5 wt% protein) prepared at pH 5 and pH 7, obtained after centrifugation.

3.3. Rheological behaviour of the emulsion-filled gels

3.3.1. Small amplitude oscillatory shear (SAOS)

To determine the effect of pH and oil concentration on the gelling properties of EFGs, the protein-enriched emulsions were subjected to a temperature sweep and the rheological behaviour was studied. Fig. 3 shows the storage modulus (G′) of the protein-enriched emulsions at different oil concentrations (10.0–30.0 wt%) and pH conditions (pH 5 and 7) as a function of time and temperature increase. It shows that even before heating, an increased oil content leads to an increased G′ at both pH 5 and 7. Upon heating an initial gradual increase in G′ was observed in the first 20 min and T < 60°C, followed by a steeper increase at 80 °C and a second slope at 100°C. The denaturation temperatures of cruciferins and napins have been reported as 80–90 and 100–110°C respectively at pH 7 (Withana-Gamage et al., 2015; Wu & Muir, 2008; J.; Yang et al., 2021) and decrease with decreasing pH (Krzyzaniak, Burova, Haertlé, & Barciszewski, 1998; Perera et al., 2016). Considering the decreased denaturation onset at pH 5, it is expected that the two slopes in the heating stage (at 80° and 100°C) correspond to the onset of denaturation of cruciferins and napins, respectively. From Fig. 3 it is also observed that upon cooling there is only a subtle increase in G′, and no gel maturation occurs during the final 5 min holding time at 20°C. At pH 5 there is also a pronounced G' increase of the heat-set gels when the oil content increases, which implies that the emulsion droplets reinforce the gel.

The situation at pH 7 is different; there is a much steeper increase in G' at the heating stage and a less pronounced slope deflection at higher temperatures. Also here the G' increases to a limited extent upon cooling, and no gel maturation occurs during the 5 min holding time at 20°C. Fig. 3 shows that the RPM forms a firmer gel (i.e. higher G') without oil at pH 7, compared with pH 5. This is consistent with what has been reported elsewhere for a rapeseed protein isolate (Tan et al., 2014). However, in our study we see that with increasing oil fraction there is less reinforcement, eventually leading to a similar G' at 30.0% oil for pH 5 and 7.

At both pH 5 and pH 7, an initial G' increase at 20–70°C was observed, which is below the denaturation onset temperatures of cruciferins and napins. It appears that a network already starts to form at these temperatures. This observation is consistent with another study on the gelling properties of rapeseed proteins, where a similar early increase of the G' was observed at pH 4 and 7 (Tan et al., 2014). We also noticed that this increase started earlier by increasing the oil concentration in the EFGs. Therefore, we hypothesize that the increase in G' at low temperatures could be caused by emulsion droplet-droplet interactions or interactions with the forming protein matrix. It is important to note that, the protein extract used in this study was freeze-dried before use. In the case that another drying method is applied on the protein extracts, such as spray-drying, the elevated temperatures above the protein denaturation temperature of the proteins might alter the structure of the proteins (Haque, Chen, Aldred, & Adhikari, 2015) and subsequently impact their gelling behaviour.

To visualize the differences in the degree of gel reinforcement in the EFGs at pH 5 and pH upon oil addition, in Fig. 4 we plotted the E_r^*, which is the G' of each EGF (G'_{EFG}) relative to the G' of the protein gel matrix (G'_{matrix}), as proposed by (van Vliet, 1988). At pH 5 the E_r^* shows a steep increase with increasing oil, whereas at pH 7 the increase is more subtle. The lower reinforcement at pH 7 with increasing oil can be possibly attributed to the higher G' of the matrix (Gravelle, Nicholson, Barbut, & Marangoni, 2019). Similar observations for gel reinforcement by oil were seen for casein emulsion-filled gels (acidified), polyvinyl alcohol – congo red gels, and whey protein isolate gels, in case the macromolecule covering the particles was selected on its ability to interact with the matrix (Dickinson & Chen, 1999; van Vliet, 1988). In more recent years, studies appeared that reconsidered existing particle reinforcement theories (Gravelle et al., 2019; Gravelle & Marangoni, 2021a, 2021b;

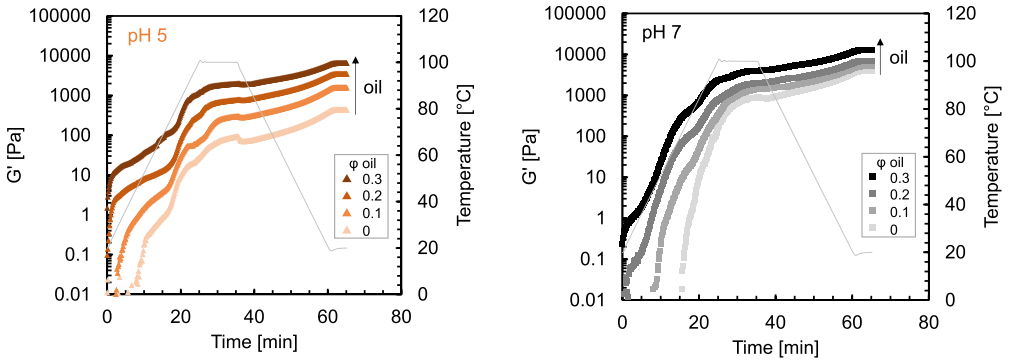

Fig. 3. Temperature sweeps of the matrix (no oil) and emulsion-filled gels with 0.1–0.3 oil mass fraction at pH 5 (left panel, orange) and 7 (right panel, black), containing 15.0 wt% rapeseed protein mixture (RPM) in the aqueous phase and oil mass fractions ranging between 0.1 and 0.3. A darker colour represents more oil. All samples were measured in duplicate and a representative curve is shown. (For interpretation of the references to colour in this figure legend, the reader is referred to the Web version of this article.)

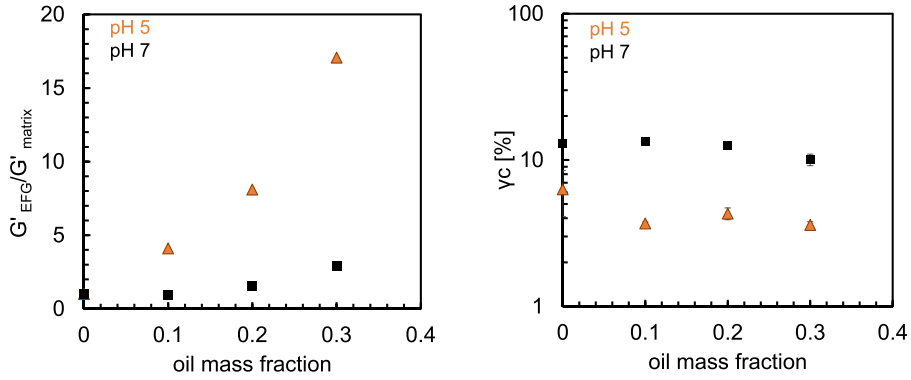

Fig. 4. Degree of reinforcement expressed as G'_{EFG}/G'_{matrix} as function of oil mass fraction (left panel) and the critical strain as function of oil mass fraction (right panel). pH 5 is represented by orange triangles and pH 7 by black squares. The critical strains are averages from duplicate measurements and the error bars represent the standard deviations. (For interpretation of the references to colour in this figure legend, the reader is referred to the Web version of this article.)

Mellema, van Opheusden, & van Vliet, 2002). In Gravelle et al. (2021b), it was proposed that at a fixed gelator concentration, E_r^* scales as:

$$E_r^* \sim (1 - \Phi_f)^{-\gamma} \quad (2)$$

With Φ_f the filler volume fraction and γ a scaling exponent. The scaling exponent γ depends on the extent of strain amplification in the matrix, as well as the correlation between the filler volume fraction and the connectivity of the load-bearing network. A higher γ value implies a larger contribution to filler reinforcement. Eq. (2) was fitted on the E_r^* data as function of filler volume fraction at pH 5 and 7. The γ at pH 5 and 7 were found to be equal to 8.04 ($R^2 = 0.97$) and 2.79 ($R^2 = 0.93$), respectively. Comparable values were seen for whey protein isolate/xanthan gum gels with glass microsphere fillers ($\gamma = 7.31$) and gelatin gels with whey protein isolate-stabilized solid fat emulsion droplets ($\gamma = 3.15$) (Gravelle & Marangoni, 2021a).

To suggest the mechanism behind the higher reinforcement observed at pH 5 compared to pH 7, additional analyses were necessary and are discussed in the following parts, where after a mechanism is proposed in section 3.5.

Apart from the effect of emulsion droplets on gel firmness, another rheological property of the gels that can be influenced by the presence of emulsion droplets is the resistance against deformation. Aiming to assess how the increase in oil concentration affects the end of the linear viscoelastic (LVE) regime of the EFGs, we determined the critical strain of the different EFGs as shown in Fig. 4. In Fig. 4 (right panel) the end of the LVE regime, expressed as a critical strain of EFGs at pH 5 and pH 7, is presented as a function of oil concentration. The critical strain was higher at pH 7 than pH 5 but remained quite constant with increasing oil concentration for both pH values, with critical strain values around 10% and 8%, respectively. In contrast to the increase in G' by oil addition as shown in Fig. 3, the extent of the LVE regime was much less affected by an increased oil content. This result shows that the structural properties of the gel protein matrix were not affected by the addition of emulsion droplets, indicating that the structural properties are mostly determined by the proteins in the gel matrix. However, this figure only provides limited information about the material's response to deformation and no information about its response beyond the LVE regime. To study the emulsion-filled gels response to large deformation, large amplitude oscillatory shear (LAOS) rheology was used.

3.3.2. *Large amplitude oscillatory shear (LAOS)*

The response of the emulsion-filled gels to non-linear deformation was studied by applying a strain sweep. At each strain amplitude the oscillatory waveform data was collected and Lissajous plots were constructed for an RPM heat-set gel (matrix) and RPM emulsion-filled gels (EFGs) with varying oil concentrations, at pH 5 and 7 at five strain amplitudes. Fig. 5 shows the elastic Lissajous plots where the normalized stress versus strain is plotted and Fig. 6 shows the viscous Lissajous plots, where the normalized stress as a function of normalized shear rate are shown. In the elastic Lissajous plots (Figs. 5) and 1% strain deformation, the gels are still within their LVE regime and show a narrow elliptical shape, indicating predominant elastic behaviour. For the viscous Lissajous plots (Fig. 6) the elastic response corresponds with a nearly circular shape. When the strain deformation increases to 50%, the elliptical shapes deflect and an overshoot of the stress at maximum strain is observed, indicating intracycle strain stiffening behaviour. At pH 5 the curves are slightly wider, which indicates that the viscous response at pH 5 becomes more dominant. This is also seen from the viscous Lissajous plots in Fig. 6, where the shapes change from circular to

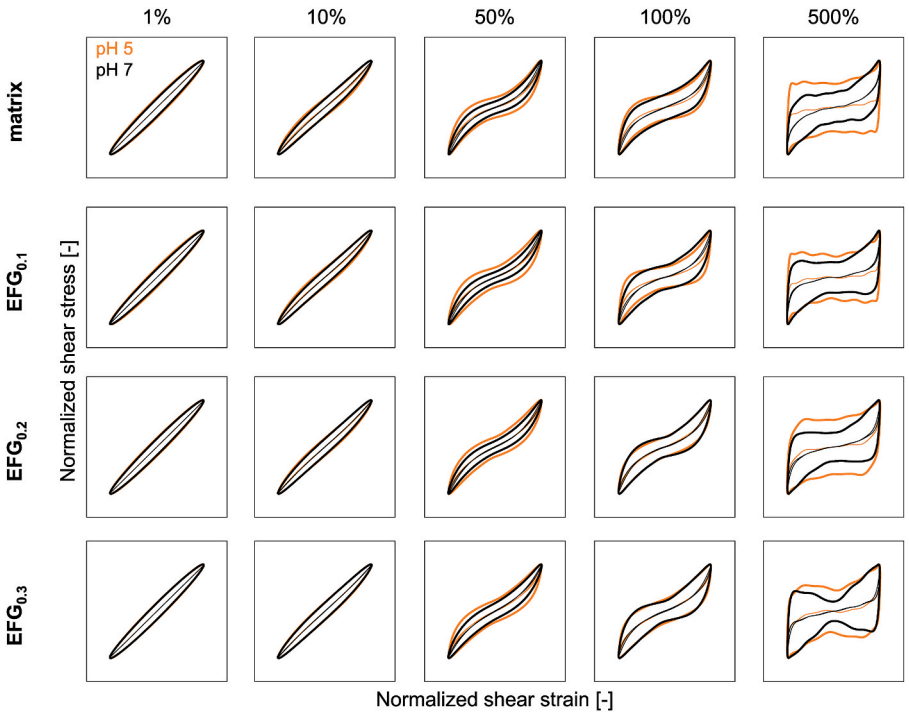

Fig. 5. Elastic Lissajous plots of normalized stress versus strain, at strain amplitudes of 1, 10, 50, 100 and 500%. The strain amplitudes were applied on the gelled matrix and emulsion-filled gels with 15.0 wt% rapeseed protein mixture (RPM) in the water phase and oil mass fractions ranging between 0.1 and 0.3. pH 5 is represented as orange and pH 7 as black. The lines within the curves represent the elastic stress contribution. (For interpretation of the references to colour in this figure legend, the reader is referred to the Web version of this article.)

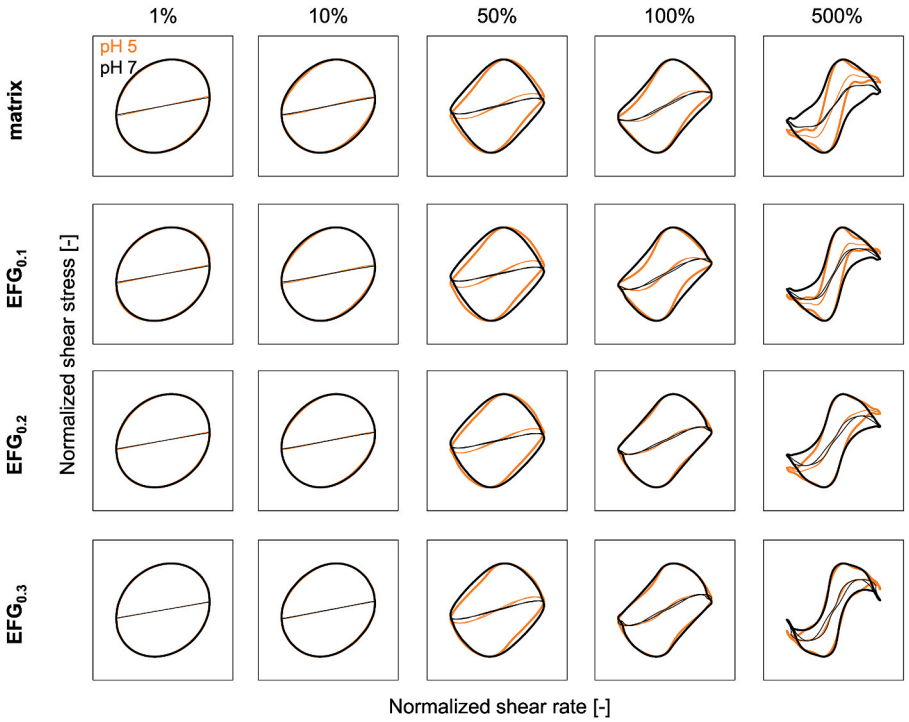

Fig. 6. Viscous Lissajous plots of normalized stress versus strain rate, at strain amplitudes of 1, 10, 50, 100 and 500%. The strain amplitudes were applied on the gelled matrix and emulsion-filled gels with 15 wt% rapeseed protein mixture (RPM) in the water phase and oil mass fractions ranging between 0.1 and 0.3. pH 5 is represented as orange and pH 7 as black. The lines within the curves represent the viscous stress contribution. (For interpretation of the references to colour in this figure legend, the reader is referred to the Web version of this article.)

rhomboidal. At 100% strain deformation the curves widen further, and the viscous response becomes more dominant at both pH 5 and 7. At 500% strain deformation the behaviour at pH 5 and 7 start to diverge. The gels at pH 5 now show a nearly rectangular shape, implying a plastic response – an initially elastic response at maximum strain, followed by yielding and flow at nearly constant stress – while the gels at pH 7 persist in their strain stiffening behaviour. The wiggles observed at pH 5, and the bowtie-like shape at pH 7 for $EFG_{0.3}$, probably result from sample or tool inertia effects coupling to the elasticity of the sample.

For a more quantitative analysis of the elastic and viscous dominated stages in the response to strain deformation, as well as the transition between them, we plotted the energy dissipation ratio as a function of strain, at a fixed frequency of 1 Hz (Fig. 7). This is the ratio of the dissipated energy within one cycle divided by the dissipation in a material displaying ideal plastic behaviour. As we already saw in the Lissajous plots, oil has little effect on the overall non-linear behaviour of the emulsion-filled gels. The results confirm that oil has hardly any effect on the breakdown behaviour of EFGs, and that the protein network

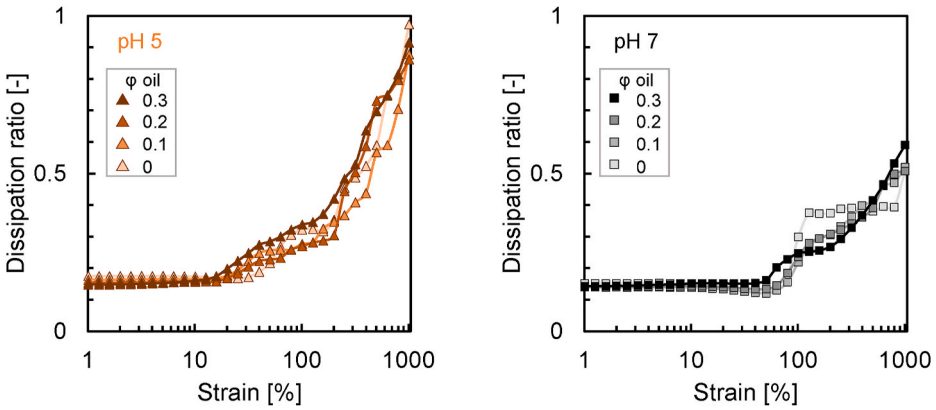

Fig. 7. The energy dissipation ratios of the gelled matrix and the emulsion-filled gels at pH 5 (left panel, orange) and 7 (right panel, black) with a constant rapeseed protein mixture (RPM) of 15.0 wt % in the aqueous phase and oil mass fractions ranging between 0.1 and 0.3. A darker colour represents more oil. All samples were measured in duplicate and a representative curve is shown. (For interpretation of the references to colour in this figure legend, the reader is referred to the Web version of this article.)

structure dictates the linear and nonlinear behaviour. The above outcome also implies that the connections between emulsion droplets and the proteins are weaker than the connections between proteins, as the emulsion droplets do not lead to an increased deformability of the gel. The pH, on the other hand, affects the non-linear behaviour of the gels. Fig. 7 shows an increase in the energy dissipation ratio already at 20% strain at pH 5, while at pH 7 the increase starts at 70% strain, which indicates that at pH 5 the EFGs are more brittle than at pH 7. The difference between pH 5 and 7 is probably related to the presence of protein aggregates initially in the system at pH 5, resulting in a weaker (lower *G'*) and more brittle gelled protein structure.

3.4. Microstructure of the emulsion-filled gels

Aiming to identify whether the differences observed in the rheological properties between the EFGs at different pH relate to differences in the microstructure of the EFGs, we used confocal laser scanning microscopy (CLSM). In Fig. 8 the micrographs of the protein matrices (top row) and EFGs with 10.0 wt% oil (bottom row) at pH 5 (left) and pH 7 (right) are displayed. At pH 5, we observed a heterogeneous protein matrix that consisted of randomly associated large protein aggregates. At pH 7, the protein matrix was more homogeneous with proteins arranged in elongated stranded-like structures. Both protein gel matrices also contained oleosomes (around 1.8 wt% of total mass), shown as spherical droplets, as RPM was extracted from non-defatted rapeseeds. Upon addition of emulsion droplets in the protein matrix, the droplets appeared to be integrated in the protein matrix both at pH 5 and pH 7, without affecting the way the matrix was structured. Here, we present the CLSM images of only the EFGs of 10.0 wt% oil, as the higher opacity of the EFGs at higher oil concentrations did not allow us to get high resolution images.

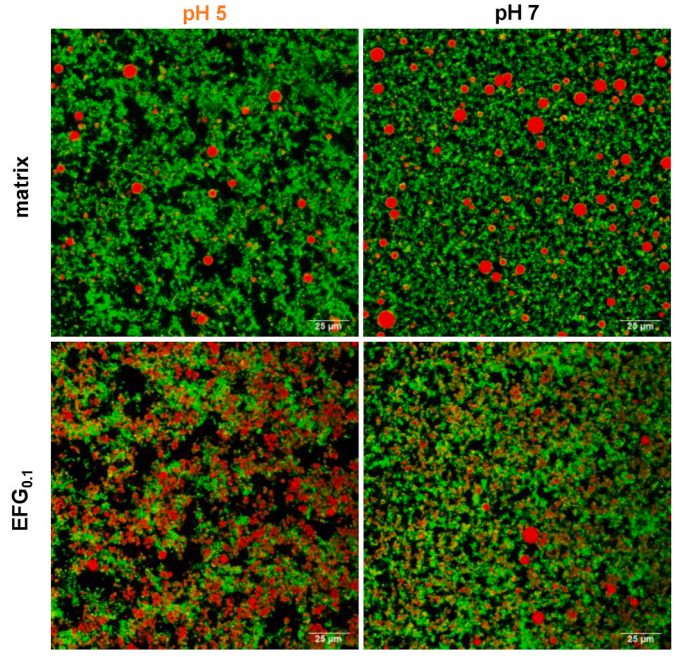

Fig. 8. CLSM images of; Top row: gelled protein matrix at pH 5 and pH 7, containing 15.0 wt% RPM where the proteins and oleosomes present are visualized, and bottom row: EFGs containing 15.0 wt% RPM and 10.0 wt% oil at pH 5 and pH 7, where the proteins and emulsion droplets are visualized. Proteins and oil are stained with Fast green and Nile red respectively. (For interpretation of the references to colour in this figure legend, the reader is referred to the Web version of this article.)

Matrix heterogeneity has been previously highlighted as an important parameter for the rheological properties of gels (Kornet et al., 2021), while the formation of particulate-like or strand-like protein gels is pH dependent (Lefevre & Subirade, 2000). At pH 5 the proteins in RPM were less soluble and pre-aggregated before heating, compared to pH 7. This pre-aggregated state resulted in a lower number of connections per unit volume of proteins (Kornet et al., 2021) and possibly partial unfolding of the proteins upon heating (Lefevre & Subirade, 2000), leading to a weaker and more heterogeneous protein network. The formation of protein strand-like structures at pH 7 could be attributed to the relatively stronger electrostatic repulsive forces between the proteins at this pH (ζ-potential around −15 mV (Ntone et al., 2020)) which could lead to a parallel arrangement of the protein polypeptide chains upon unfolding, with increased intermolecular interactions (Lefevre & Subirade, 2000). This arrangement in turn resulted in a more homogeneous and firmer protein network (higher G').

3.5. Mechanistic understanding for gel reinforcement by the presence of emulsion droplets

It was found that the presence of emulsion droplets reinforces the gel firmness of rapeseed protein mixture (RPM) gels and that the reinforcement was more pronounced at pH 5 than pH 7. To propose a mechanism behind this reinforcement, there are three factors to consider.

The first factor is whether the interface of the emulsion droplets interact with the matrix, which determines whether a filler is active or inactive (Farjami & Madadlou, 2019). Earlier research showed that napins dominate the oil droplet interface in emulsions stabilized by RPM, as a result of their small size and Janus-like conformation. Furthermore, cruciferins appeared to weakly interact with the interfacial layer of napins (Ntone et al., 2021). The napin-cruciferin interactions at the emulsion droplet-matrix interface suggest that the napin-stabilized emulsion droplets can be present as active fillers in a protein network built by cruciferins.

The second factor to consider is the stiffness of the droplets relative to the matrix, which can be expressed by the M ratio:

$$M = \frac{G'_{filler}}{G'_{matrix}} \quad (3)$$

When $M < 1$ the matrix is stiffer than the filler, and when $M > 1$ the emulsion droplets (fillers) are stiffer than the matrix. Given that stiffer droplets can interact with the matrix (active fillers), the gel structure can be reinforced (Geremias-Andrade et al., 2016; Sala, 2007; van Vliet, 1988). The G' of the matrix was measured, and the G' of the filler can be approximated by estimating the Laplace pressure

$$G'_{filler} = \frac{2\sigma}{r} \quad (4)$$

which is an expression based on van Vliet (1988). In its original form, this expression is based on the surface tension (σ) of the oil-water interface, which is appropriate for interfaces stabilized by low molecular weight surfactants. Here, as the interface was stabilized by proteins – which form interfaces with a predominantly viscoelastic solid-like behaviour – the surface tension was replaced by the dilatational elastic modulus (E_d').

In earlier research (Ntone et al., 2021) the dilatational elastic modulus was found to be around 25 mN/m, and the average droplet size of the emulsions ($d_{4,3}$) was around 2 μm as shown in Table 1. Taking into account these values the estimated G'_{filler}, and the measured G' values for the RPM matrix at pH 5 and 7 were used to determine the M ratio. The M ratios were 126 and 12 at pH 5 and 7, respectively. This indicates that the emulsion droplets were stiffer than the matrix, and thus would have the potential to reinforce emulsion-filled gels. Considering that the stiffer napin-stabilized droplets interact with the protein matrix as suggested earlier, they can reinforce the gel firmness by increasing the number of connections per unit volume of the protein network. The 10-fold higher M ratio at pH 5 compared to pH 7 (126 vs 12) also indicates that the emulsion droplets are significantly much stiffer (higher G'_{filler}) than the protein matrix at pH 5 compared to pH 7. This difference can also justify the higher degree of reinforcement observed at pH 5 after the addition of emulsion droplets.

The third factor to consider is the matrix microstructure. In the CLSM images (Fig. 8), we showed that at pH 5 gels with higher heterogeneity built of protein aggregates were formed, whereas at pH 7 the gels had a more homogeneous structure built of protein strands. The same microstructure was observed upon addition of emulsion droplets. It has been previously reported that in EFGs, a higher degree of matrix heterogeneity results in a larger gel reinforcement effect by addition of oil, compared to more homogeneous gels (Oliver, Wieck, & Scholten, 2016). The suggested explanation for this increase is the accumulation of the dispersed droplets in the protein-poor regions of heterogeneous protein matrices, increasing the effective volume fraction of the droplets (Oliver et al., 2016).

The higher degree of gel heterogeneity observed here at pH 5 can also justify the higher reinforcement of the gel firmness observed at pH 5 compared to pH 7. However, in contrast to the suggested changes in the gel structure by oil addition in the aforementioned study (i.e. accumulation of droplets) (Oliver et al., 2016), in the CLSM images (Fig. 8) we did not observe any changes in the type of protein gel network (i.e. aggregates or strands) or changes in the heterogeneity or homogeneity of the structure upon addition of emulsion droplets, neither at pH 5 nor pH 7. The unchanged microstructure of EFGs in addition to the unchanged critical strain or response of the gel structure to large deformations upon addition of emulsion droplets, suggests that the microstructure of the protein matrix and the EFGs is dictated by protein-protein interactions.

Therefore, the added emulsion droplets, being stiffer than the protein matrix and integrated in the structural matrix, increased the gel firmness. The rheological data, combined with CLSM images, also give some insight into how the gel network is built on a microscale. According to the scaling model developed by Shih, Shih, Kim, Liu, and Aksay (1990), the gel structure can be classified by two regimes, in which either the inter- or intra-floc links are stronger (Shih et al., 1990). In a weak-link regime, the inter-floc links are weaker than the intra-floc links, whereas in a strong-link regime the inter-floc links are stronger than the intra-floc links (Shih et al., 1990). The confocal microscopy images suggested that emulsion droplets were incorporated within the protein network and did not alter the protein matrix structure. Moreover, the rheological data showed that the breakdown behaviour of the gels did not change upon the addition of emulsion droplets, as the γ_0 was hardly affected by an increased oil content. Both data imply that the inter-flock links between the droplets and the protein matrix were not very strong, leading to the hypothesis that RPM forms weak-link gels.

4. Conclusions

We showed that when napins and cruciferins are both present in a less purified rapeseed protein mixture, they can have complementary roles in structuring EFGs, with napins stabilizing the emulsion droplets and cruciferins building the protein network. In the emulsion-filled gels, pH played an important role in the type of protein network formed upon gelation; at pH 5 a more heterogeneous protein network and less firm emulsion-filled gels were formed compared to pH 7, possibly due to the higher pre-aggregated state of cruciferins at pH 5. Independent of pH, the presence of emulsion droplets led to increase of the gel firmness with more pronounced effects at low pH. The mechanism of reinforcement of EFGs by the presence of emulsion droplets is attributed to the fact that the added emulsion droplets were stiffer than the protein matrix, and integrated in the structural matrix, increasing the gel firmness. Our results can inspire food manufacturers and scientists to exploit the potential complementary functionalities of various extracted plant proteins to create multi-functional ingredients that can enhance the performance of plant-based foods.

Author statement

Eleni Ntone: Conceptualization, Methodology, Investigation, Validation, Formal Analysis, Visualization, Writing – Original Draft, Remco Kornet: Conceptualization, Methodology, Investigation, Validation, Formal Analysis, Visualization, Writing – Original Draft, Paul Venema: Supervision, Methodology, Conceptualization, Writing – Review & Editing, Marcel Meinders: Funding Acquisition, Writing – Review & Editing, Erik van der Linden: Funding Acquisition, Writing – Review & Editing, Johannes H. Bitter: Writing - review & editing, Leonard M.C. Sagis: Supervision, Methodology, Conceptualization, Writing - review & editing, Constantinos V. Nikiforidis; Conceptualization; Supervision; Validation; Methodology; Project administration; Writing - review & editing.

Declaration of competing interest

None.

Acknowledgements

The authors thank Dr. Philipp Fuhrmann for sharing his expertise in the field of oil droplet clustering and providing us with practical suggestions. The project is organised by and executed under the auspices of TiFN, a public -private partnership on precompetitive research in food and nutrition. The authors have declared that no competing interests exist in the writing of this publication. Funding for this research was obtained from Unilever Research and Development Wageningen, Nutricia Research B·V., Bel group, Pepsico Inc., the Netherlands Organisation for Scientific Research (ALWTF.2016.024) and the Top-sector Agri&Food.

References

Assatory, A., Vitelli, M., Rajabzadeh, A. R., & Legge, R. L. (2019). Dry fractionation methods for plant protein, starch and fiber enrichment: A review. November 2018 *Trends in Food Science & Technology, 86*, 340–351. https://doi.org/10.1016/j.tifs.2019.02.006.

Berghout, J. A. M., Pelgrom, P. J. M., Schutyser, M. A. I., Boom, R. M., & Van Der Goot, A. J. (2015). Sustainability assessment of oilseed fractionation processes: A case study on lupin seeds. *Journal of Food Engineering, 150*, 117–124. https://doi.org/10.1016/j.jfoodeng.2014.11.005

Braun, D. D., & Rosen, M. R. (2013). *Rheology modifiers handbook: Practical use and application*. Elsevier.

Chen, J., & Dickinson, E. (1998). Viscoelastic properties of heat-set whey protein emulsion gels. *Journal of Texture Studies, 29*(3), 285–304. https://doi.org/10.1111/j.1745-4603.1998.tb00171.x

Chen, J., & Dickinson, E. (1999). Effect of surface character of filler particles on rheology of heat-set whey protein emulsion gels. *Colloids and Surfaces B: Biointerfaces, 12*(3–6), 373–381. https://doi.org/10.1016/S0927-7765(98)00091-5

Chen, J., Dickinson, E., & Edwards, M. (1999). Rheology of acid-induced sodium caseinate stabilized emulsion gels. *Journal of Texture Studies*. https://doi.org/10.1111/j.1745-4603.1999.tb00226.x

Cheung, L., Wanasundara, J. P. D., & Nickerson, M. T. (2014). The effect of pH and NaCl levels on the physicochemical and emulsifying properties of a cruciferin protein isolate. *Food Biophysics, 9*(2), 105–113. https://doi.org/10.1007/s11483-013-9323-2

Chmielewska, A., Kozłowska, M., Rachwał, D., Wnukowski, P., Amarowicz, R., Nebesny, E., et al. (2020). Canola/rapeseed protein–nutritional value, functionality and food application: A review, 0(0) *Critical Reviews in Food Science and Nutrition*, 1–21. https://doi.org/10.1080/10408398.2020.1809342.

Dalgalarrondo, M., Robin, J. M., & Azanza, J. L. (1986). Subunit composition of the globulin fraction of rapeseed (Brassica napus L.). *Plant Science, 43*, 115–124. https://doi.org/10.1016/0168-9452(86)90151-2

Dickinson, E. (2012). Emulsion gels: The structuring of soft solids with protein-stabilized oil droplets. *Food Hydrocolloids, 28*(1), 224–241. https://doi.org/10.1016/j.foodhyd.2011.12.017

Dickinson, E. (2014). Understanding food structures: The colloid science approach. In *Food Structures, Digestion and Health*. Elsevier Inc. https://doi.org/10.1016/B978-0-12-404610-8.00001-3.

Dickinson, E., & Chen, J. (1999). Heat-set whey protein emulsion gels: Role of active and inactive filler particles. *Journal of Dispersion Science and Technology, 20*(1–2), 197–213. https://doi.org/10.1080/01932699908943787

Dickinson, E., & Hong, S. T. (1995). Influence of water-soluble nonionic emulsifier on the rheology of heat-set protein-stabilized emulsion gels. *Journal of Agricultural and Food Chemistry, 43*(10), 2560–2566. https://doi.org/10.1021/jf00058a002

Ewoldt, R. H., Winter, P., Maxey, J., & McKinley, G. H. (2010). Large amplitude oscillatory shear of pseudoplastic and elastoviscoplastic materials. *Rheologica Acta, 49*(2), 191–212. https://doi.org/10.1007/s00397-009-0403-7

Farjami, T., & Madadlou, A. (2019). An overview on preparation of emulsion-filled gels and emulsion particulate gels. April 2018 *Trends in Food Science & Technology, 86*, 85–94. https://doi.org/10.1016/j.tifs.2019.02.043.

Fetzer, A., Herfellner, T., Stäbler, A., Menner, M., & Eisner, P. (2018). Influence of process conditions during aqueous protein extraction upon yield from pre-pressed and cold-pressed rapeseed press cake. *Industrial Crops and Products, 112*, 236–246. https://doi.org/10.1016/j.indcrop.2017.12.011

Fuhrmeister, H., & Meuser, F. (2003). Impact of processing on functional properties of protein products from wrinkled peas. *Journal of Food Engineering, 56*(2–3), 119–129. https://doi.org/10.1016/S0260-8774(02)00241-8

Genovese, D. B. (2012). Shear rheology of hard-sphere, dispersed, and aggregated suspensions, and filler-matrix composites. *Advances in Colloid and Interface Science, 171–172*, 1–16. https://doi.org/10.1016/j.cis.2011.12.005

Geremias-Andrade, I., Souki, N., Moraes, I., & Pinho, S. (2016). Rheology of emulsion-filled gels applied to the development of food materials. *Gels, 2*(3), 22. https://doi.org/10.3390/gels2030022

Gerzhova, A., Mondor, M., Benali, M., & Aider, M. (2016). Study of total dry matter and protein extraction from canola meal as affected by the pH, salt addition and use of zeta-potential/turbidimetry analysis to optimize the extraction conditions. *Food Chemistry, 201*, 243–252. https://doi.org/10.1016/j.foodchem.2016.01.074

Gravelle, A. J., & Marangoni, A. G. (2021a). A new fractal structural-mechanical theory of particle-filled colloidal networks with heterogeneous stress translation. *Journal of Colloid and Interface Science, 598*, 56–68. https://doi.org/10.1016/j.jcis.2021.03.180

Gravelle, A. J., & Marangoni, A. G. (2021b). Effect of matrix architecture on the elastic behavior of an emulsion-filled polymer gel. February *Food Hydrocolloids, 119*. https://doi.org/10.1016/j.foodhyd.2021.106875.

Gravelle, A. J., Nicholson, R. A., Barbut, S., & Marangoni, A. G. (2019). Considerations for readdressing theoretical descriptions of particle-reinforced composite food gels. April *Food Research International, 122*, 209–221. https://doi.org/10.1016/j.foodres.2019.03.070.

Haque, M. A., Chen, J., Aldred, P., & Adhikari, B. (2015). Drying and denaturation characteristics of whey protein isolate in the presence of lactose and trehalose. *Food Chemistry, 177*, 8–16. https://doi.org/10.1016/j.foodchem.2014.12.064

Karefyllakis, D., Octaviana, H., van der Goot, A. J., & Nikiforidis, C. V. (2019). The emulsifying performance of mildly derived mixtures from sunflower seeds. *Food Hydrocolloids, 88*, 75–85. https://doi.org/10.1016/j.foodhyd.2018.09.037

Kornet, R., Veenemans, J., Venema, P., Jan, A., Goot, V. Der, Meinders, M., et al. (2021). Less is more : Limited fractionation yields stronger gels for pea proteins. *Food Hydrocolloids, 112*, 106285. https://doi.org/10.1016/j.foodhyd.2020.106285

Krause, J. P., & Schwenke, K. D. (2001). Behaviour of a protein isolate from rapeseed (Brassica napus) and its main protein components - globulin and albumin - at air/solution and solid interfaces, and in emulsions. *Colloids and Surfaces B: Biointerfaces, 21*(1–3), 29–36. https://doi.org/10.1016/S0927-7765(01)00181-3

Krzyzaniak, A., Burova, T., Haertlé, T., & Barciszewski, J. (1998). The structure and properties of Napin-seed storage protein from rape (Brassica napus L.). *Nahrung-Food*. https://doi.org/10.1002/(sici)1521-3803(199808)42:03/04<201::aid-food201>3.3.co;2-l

Lefevre, T., & Subirade, M. (2000). Molecular differences in the formation and structure of fine-stranded and particulate β-lactoglobulin gels. *Biopolymers, 54*, 578–586. https://doi.org/10.1002/1097-0282(200012)54:7<578::AID-BIP100>3.0.CO;2-2

Lie-Piang, A., Braconi, N., Boom, R. M., & van der Padt, A. (2021). Less refined ingredients have lower environmental impact – a life cycle assessment of protein-rich ingredients from oil- and starch-bearing crops. *Journal of Cleaner Production, 292*. https://doi.org/10.1016/j.jclepro.2021.126046

Loveday, S. M. (2020). Plant protein ingredients with food functionality potential. *Nutrition Bulletin, 45*(3), 321–327. https://doi.org/10.1111/nbu.12450

McClements, D. J., Monahan, F. J., & Kinsella, J. E. (1993). Effect of emulsion droplets on the rheology of whey protein isolate gels. *Journal of Texture Studies, 24*(4), 411–422. https://doi.org/10.1111/j.1745-4603.1993.tb00051.x

McCurdy, S. M. (1990). Effects of processing on the functional properties of canola/rapeseed protein. *Journal of the American Oil Chemists' Society, 67*(5), 281–284. https://doi.org/10.1007/BF02539677

Mellema, M., van Opheusden, J. H. J., & van Vliet, T. (2002). Categorization of rheological scaling models for particle gels applied to casein gels. *Journal of Rheology, 46*(1), 11–29. https://doi.org/10.1122/1.1423311

Monsalve, R. I., Lopez-otin, C., Villalba, M., & Rodriguez, R. (1991). A new distinct group of 2 S albumins from rapeseed: Amino acid sequence of two low molecular weight napins. *FEBS Letters, 295*(1), 207–210.

Mosenthin, R., Messerschmidt, U., Sauer, N., Carré, P., Quinsac, A., & Schöne, F. (2016). Effect of the desolventizing/toasting process on chemical composition and protein quality of rapeseed meal. *Journal of Animal Science and Biotechnology, 7*(1), 1–12. https://doi.org/10.1186/s40104-016-0095-7

Ntone, E., Bitter, J. H., & Nikiforidis, C. V. (2020). Not sequentially but simultaneously: Facile extraction of proteins and oleosomes from oilseeds. *Food Hydrocolloids, 102*, 105598. https://doi.org/10.1016/j.foodhyd.2019.105598

Ntone, E., van Wesel, T., Sagis, L. M. C., Meinders, M., Bitter, J. H., & Nikiforidis, C. V. (2021). Adsorption of rapeseed proteins at oil/water interfaces. Janus-like napins dominate the interface. *Journal of Colloid and Interface Science, 583*, 459–469. https://doi.org/10.1016/j.jcis.2020.09.039

Oliver, L., Wieck, L., & Scholten, E. (2016). Influence of matrix inhomogeneity on the rheological properties of emulsion-filled gels. *Food Hydrocolloids, 52*, 116–125. https://doi.org/10.1016/j.foodhyd.2015.06.003

Ozdal, T., Capanoglu, E., & Altay, F. (2013). A review on protein-phenolic interactions and associated changes. *Food Research International, 51*(2), 954–970. https://doi.org/10.1016/j.foodres.2013.02.009

Papalamprou, E. M., Doxastakis, G. I., Biliaderis, C. G., & Kiosseoglou, V. (2009). Influence of preparation methods on physicochemical and gelation properties of chickpea protein isolates. *Food Hydrocolloids, 23*(2), 337–343. https://doi.org/10.1016/j.foodhyd.2008.03.006

Peng, Y., Kersten, N., Kyriakopoulou, K., & van der Goot, A. J. (2020). Functional properties of mildly fractionated soy protein as influenced by the processing pH. *Journal of Food Engineering, 275*, 109875. https://doi.org/10.1016/j.jfoodeng.2019.109875

Perera, S., McIntosh, T., & Wanasundara, J. P. D. (2016). Structural properties of cruciferin and napin of Brassica napus (Canola) show distinct responses to changes in pH and temperature. *Plants, 5*(3), 36. https://doi.org/10.3390/plants5030036

Rawel, H. M., Meidtner, K., & Kroll, J. (2005). Binding of selected phenolic compounds to proteins. *Journal of Agricultural and Food Chemistry, 53*(10), 4228–4235. https://doi.org/10.1021/jf0480290

Reynoldst, J. A., & Tanford, C. (1970). Binding of dodecyl sulfate to proteins at high binding ratios. Possible implications for the state of proteins in biological membranes. *Proceedings of the National Academy of Sciences of the United States of America, 66*(3), 1002–1003. https://doi.org/10.1073/pnas.66.3.1002

Rubino, M. I., Arntfield, S. D., Nadon, C. A., & Bernatsky, A. (1996). Phenolic protein interactions in relation to the gelation properties of canola protein. *Food Research International, 29*(7), 653–659. https://doi.org/10.1016/S0963-9969(97)89643-3

Sala, G. (2007). *Food gels filled with emulsion droplets linking large deformation properties to sensory perception* (PhD Thesis). Wageningen University.

Sala, G., van Vliet, T., Cohen Stuart, M. A., Aken, G. A. va, & van de Velde, F. (2009a). Deformation and fracture of emulsion-filled gels: Effect of oil content and deformation speed. *Food Hydrocolloids, 23*(5), 1381–1393. https://doi.org/10.1016/j.foodhyd.2008.11.016

Sala, G., van Vliet, T., Cohen Stuart, M., van de Velde, F., & van Aken, G. A. (2009b). Deformation and fracture of emulsion-filled gels: Effect of gelling agent concentration and oil droplet size. *Food Hydrocolloids, 23*(7), 1853–1863. https://doi.org/10.1016/j.foodhyd.2009.03.002

Sari, Y. W., Mulder, W. J., Sanders, J. P. M., & Bruins, M. E. (2015). Towards plant protein refinery: Review on protein extraction using alkali and potential enzymatic assistance. *Biotechnology Journal, 10*(8), 1138–1157. https://doi.org/10.1002/biot.201400569

Schreuders, F. K. G., Sagis, L. M. C., Bodnár, I., Erni, P., Boom, R. M., & van der Goot, A. J. (2021). Small and large oscillatory shear properties of concentrated proteins. *Food Hydrocolloids, 110*, 106172. https://doi.org/10.1016/j.foodhyd.2020.106172

Schutyser, M. A. I., & van der Goot, A. J. (2011). The potential of dry fractionation processes for sustainable plant protein production. *Trends in Food Science & Technology, 22*(4), 154–164. https://doi.org/10.1016/j.tifs.2010.11.006

Schwenke, K. D., Dahme, A., & Wolter, T. (1998). Heat-induced gelation of rapeseed proteins: Effect of protein interaction and acetylation. *Journal of the American Oil Chemists Society, 75*(1), 83–87. https://doi.org/10.1007/s11746-998-0015-x

Shih, W., Shih, Y., Kim, S., Liu, J., & Aksay, I. A. (1990). Scaling behavior of the elastic properties of colloidal gels. *Physical Review A, 42*(8). https://doi.org/10.1103/PhysRevA.42.4772

Sridharan, S., Meinders, M. B. J., Bitter, H. J., & Nikiforidis, C. V. (2020). Pea flour as stabilizer of oil-in-water emulsions: No protein purification necessary. *Food Hydrocolloids, 101*, 105533. https://doi.org/10.1016/j.foodhyd.2019.105533

Tamayo Tenorio, A., Kyriakopoulou, K. E., Suarez-Garcia, E., van den Berg, C., & van der Goot, A. J. (2018). Understanding differences in protein fractionation from conventional crops, and herbaceous and aquatic biomass - consequences for industrial use. December 2017 *Trends in Food Science & Technology, 71*, 235–245. https://doi.org/10.1016/j.tifs.2017.11.010.

Tan, S. H., Mailer, R. J., Blanchard, C. L., Agboola, S. O., & Day, L. (2014). Gelling properties of protein fractions and protein isolate extracted from Australian canola meal. *Food Research International, 62*, 819–828. https://doi.org/10.1016/j.foodres.2014.04.055

Van Der Goot, A. J., Pelgrom, P. J. M., Berghout, J. A. M., Geerts, M. E. J., Jankowiak, L., Hardt, N. A., et al. (2016). Concepts for further sustainable production of foods. *Journal of Food Engineering, 168*, 42–51. https://doi.org/10.1016/j.jfoodeng.2015.07.010

van Vliet, T. (1988). Rheological properties of filled gels. Influence of filler matrix interaction. *Colloid & Polymer Science, 266*(6), 518–524. https://doi.org/10.1007/BF01420762

Wanasundara, J. P. D., Abeysekara, S. J., McIntosh, T. C., & Falk, K. C. (2012). Solubility differences of major storage proteins of brassicaceae oilseeds. *Journal of the American Oil Chemists' Society, 89*(5), 869–881. https://doi.org/10.1007/s11746-011-1975-9

Wanasundara, J. P. D., McIntosh, T. C., Perera, S. P., Withana-Gamage, T. S., & Mitra, P. (2016). Canola/rapeseed protein-functionality and nutrition. *Ocl, 23*(4), D407. https://doi.org/10.1051/ocl/2016028

Withana-Gamage, T. S., Hegedus, D. D., Qiu, X., & Wanasundara, J. P. D. (2015). Solubility, heat-induced gelation and pepsin susceptibility of cruciferin protein as affected by subunit composition. *Food Biophysics, 10*(2), 103–115. https://doi.org/10.1007/s11483-014-9370-3

Wu, J., & Muir, A. D. (2008). Comparative structural, emulsifying, and biological properties of 2 major canola proteins, cruciferin and napin. *Journal of Food Science, 73*(3). https://doi.org/10.1111/j.1750-3841.2008.00675.x

Yang, J., Faber, I., Berton-Carabin, C. C., Nikiforidis, C. V., van der Linden, E., & Sagis, L. M. C. (2021). Foams and air-water interfaces stabilised by mildly purified rapeseed proteins after defatting. *Food Hydrocolloids, 112*, 106270. https://doi.org/10.1016/j.foodhyd.2020.106270

Yang, C., Wang, Y., Vasanthan, T., & Chen, L. (2014). Impacts of pH and heating temperature on formation mechanisms and properties of thermally induced canola protein gels. *Food Hydrocolloids, 40*, 225–236. https://doi.org/10.1016/j.foodhyd.2014.03.011